Journal of Applied Fluid Mechanics, Vol. 11, No. 6, pp. 1531-1541, 2018.
Available online at www.jafmonline.net, ISSN 1735-3572, EISSN 1735-3645.
DOI: 10.29252/jafm.11.06.28283

Optimization of an Active Electrokinetic Micromixer Based on the Number and Arrangement of Microelectrodes

B. Keshavarzian[1†], M. Shamshiri[2], M. Charmiyan[3] and A. Moaveni[4]

[1] *Department of Mechanical Engineering, Borujerd Branch, Islamic Azad University, Borujerd, Iran*
[2] *Department of Mechanical Engineering, McGill University, Montreal, QC H3A 0C3, Canada*
[3] *Department of Mechanical Engineering, University of Ayatollah Ozma Borujerdi, Borujerd, Iran*
[4] *Department of Mechanical Engineering, Isfahan University of Technology, Isfahan, 84156-83111, Iran*

†*Corresponding Author Email: b.keshavarzian@iaub.ac.ir*

(Received July 31, 2017; accepted May 20, 2018)

ABSTRACT

This paper reports enhancement of mixing process via electroosmotic phenomenon using a microelectrode system, which is structured by aligning a number of electrodes placed on the walls of a mixing chamber integrated within a T-Shape micromixer. A number of electrodes are dispositioned on the inner and outer loops of the annular mixing chamber, and different design patterns based on a variety of arrangements for these electrodes are investigated using numerical methods. The electric potentials on the microelectrodes are time-dependent, and this is found to be a key element for chaotic mixing. Also, it is deduced that due to the impact of the applied AC electric field and the induced surface charge on the fluid particles, a number of vortices are generated in the aqueous solution. These vortices significantly enhance the mixing of the species in the mixing chamber. In order to find an optimum pattern based on electrode dispositioning and the number of electrodes, effects of the geometric configuration of the microelectrodes are analyzed and the mixing effects for different design patterns are investigated via comparing the associated flow structure, concentration transport mechanism, and the mixing performance. Analyzing different designs, an optimum pattern based on the electrode arrangement and the number of electrodes is found to be the case for which the electrodes are placed on the inner and outer loops of the mixing chamber in a cross-like pattern.

Keywords: Mixing process; Electrokinetic excitation; Computation; Optimization.

NOMENCLATURE

c	concentration of diffusing species
c_0	initial concentration of the species
c_∞	ideal value of concentration
D	diffusion coefficient of the solution
$\mathbf{E}$	bulk electric field
f	frequency applied to the electrodes
L	channel length
L_c	characteristic length
$\mathbf{n}$	unit vector normal to the boundary
p	pressure
R	radius of the chamber
t	time
$\mathbf{u}$	velocity vector
U_0	mean inflow velocity
V	electric potential
V_0	amplitude of the applied voltage
ε_r	relative permittivity of the fluid
Γ_m	mixing efficiency
η	dynamic viscosity η
λ	reaction rate
λ_D	double layer thickness
ρ	density
σ	conductivity of the ionic solution
ζ	zeta potential

1. INTRODUCTION

In many microfluidic applications, e.g., fast chemical reactions, DNA separation and amplification, efficient microfluidic mixing schemes are required to ensure that a thorough species mixing can be achieved within small space

and time scales. Micromixers are microfluidic systems which enable mixing two or several fluids into a homogenous solution, or control the dispersion of species in solvents (Karniadakis *et al.* 2005; Nguyen and Wu 2005; Suh and Kang 2010; Lee *et al.* 2011; Stevens *et al.* 2012; Baheri Islami and Khezerloo 2017). Micromixers are often classified into two broad categories based on their operation mechanism: passive and active mixers. Passive micromixers do not need external actuating forces to operate, and mixing of fluids within them occurs by changing the design and structure of the channels. The operation principle of the passive-type mixers is mainly based on fluid stretch, folding, breakup, and molecular diffusion. These mixers, however, require long mixing time and length to achieve uniform and complete mixing, and may be fabricated as part of the microfluidic chip with reduced complexity. Obviously, this mixing efficiency cannot be accepted in practical use. To reduce the mixing lengths (the diffusion path between fluid streams) in passive micromixers, some designs based on techniques such as chaotic advection, splitting/recombination, lamination, and Dean vortices are proposed (Sudarsan and Ugaz 2006; Tofteberg *et al.* 2010; Li *et al.* 2012). In contrast, active micromixers either use moving components or employ external forcing/energy sources such as pressure (Glasgow and Aubry 2003), temperature (Mao *et al.* 2002), magnetohydrodynamics (Qian *et al.* 2002; Qian and Bau 2005, 2009), acoustics/ultrasonics (Zhu and Kim 1997; Yang *et al.* 2001), and electrokinetics (Jacobson *et al.* 1999; Oddy *et al.* 2001; Xuan and Li 2004; Wu and Li 2008; Lim *et al.* 2010; Daghighi and Li 2013) to enhance mixing performance through perturbing the flow field. In comparison with their passive counterparts, active mixers require shorter mixing time and distance to complete mixing processes and also, provide the possibility to switch the mixing process to off/on status in case of necessity. Recent research has focused on reducing the possible complexity which may be added the overall design due to integration of this type of actuators into the system.

Electroosmosis, is referred to as motion of ionized liquids relative to stationary charged surfaces, caused by an applied electric field. This electrokinetic phenomenon enhances mixing through perturbing the flow field in microchannels and promoting flow patterns like that of turbulent flows. The simplicity of the electroosmotic mixing method has attracted much attention in the fields of microfluidics and LOC (Ramos *et al.* 2003; Olesen *et al.* 2006). For such an induced-charge electrokinetic phenomenon, disturbance of the laminar flow field for vortex generation can be achieved by applying either AC (Oddy *et al.* 2001; Boy and Storey 2007; Stoeber *et al.* 2007), or DC (Biddiss *et al.* 2004; Wu and Li 2008; Ng *et al.* 2009) electric fields. Many numerical and experimental studies have been performed to induce perturbation to a liquid flowing through a microchannel (Wu and Li 2008a,b; Jain *et al.* 2009; Campisi *et al.* 2009; Ye and Li 2004). Generally, AC-micromixers require manipulation of electrical excitation parameters such as voltage, frequency and duty cycle as well as optimal design of the structure of the micromixer and the shape and position of the electrodes to deliver the best possible performance. Hence, many studies of the electrokinetic mixing in microchannels are focused on applying AC electric fields and investigating the optimized design for AC-micromixers based on the already-mentioned influential design parameters. Sasaki *et al.* (2010) developed an electroosmotic micromixer the bottom surface of which is mounted with a pair of electrodes with a sinusoidal inter electrode gap. AC voltage was applied to the electrodes and frequency was varied from 1 to 5 KHz. The maximum mixing efficiency of over 90% percent was achieved at 1 KHz. Huang *et al.* (2007) designed a novel electroosmotic micromixer with different electrode configurations on the bottom surface of the mixing channel, which generated microvortex patterns in steady state. Proposing a dc-biased AC Electroosmotic micromixer which utilizes asymmetric vortex flows for mixing, Park *et al.* (2012) reported the dependence of mixing index on the number of electrode pairs. They showed that both flow rate and number of electrode pairs influence the development of vortex flows and thereby, the mixing efficiency. They also found that for a specified flow rate, there may be a proper number of electrode pairs which gives the best mixing performance. Using microchannel with T-type electrodes, Chen *et al.* (2009) investigated performance of an AC-micromixer based on factors such as capacitive charging, Faradaic charging and asymmetric polarization, and reported an improved mixing effect regarding these three different protocols. Chen *et al.* (2003) and Zhang *et al.* (2004) designed, analyzed, and fabricated a novel AC electroosmotic micromixer with a ring-shape mixing chamber equipped with microelectrodes to promote mixing of microfluids by oscillating electroosmotic excitation. Four symmetrically located microelectrodes integrated at the outer wall of the central circular loop are used to apply a time-varying electrical field. It has been shown that the silicon-fabricated micromixer with MEMS technology which has no moving parts is an effective miniaturized device for chaotic mixing.

Mathematical modeling plays a key role in achieving an understanding of the flow structure and mixing mechanisms which, in turn, is a requirement for optimization of mixing processes. Computational fluid dynamics (CFD) has been widely employed to enhance the design of micromixers. The demand for optimized microfluidic devices in LOC applications is so high that there is a need for further simulation and optimization studies on existing and new micromixers. The present study aims at optimizing the original electroosmotic micromixer design presented by Chen *et al.* (2003) and Zhang *et al.* (2004) based on configuration of the electrodes placed on the walls of the mixing chamber to find the electrode arrangement that delivers the best mixing products. Hence, in this study, we investigate microfluidic mixing in a chaotic electrokinetic T-shape annular micromixer for a

variety of geometric models with different number and arrangement of the electrodes. This electroosmotic microchannel mixer utilizes heterogeneous surface potential to form recirculation flow and enhance mixing of the species. Here, both electroosmosis phenomenon and splitting/recombination technique are considered to enhance the degree of mixing of the agents. The main purpose of this study is to systematically identify the optimal design with regard to the arrangement of the electrodes which delivers the best performance and mixing products among the possible options. Here, multiphysics (fluid flow, electrical, and concentration fields) in the micromixer is studied via numerical simulation using the finite element based software COMSOL Multiphysics. A numerical strategy has been employed to evaluate the transport quantities associated with the AC electroosmotic flow and solution transport within the micromixers. In the first step, a stationary solver is developed by overriding the time-dependency of the system which allows to achieve a steady solution by solving for the transport variables. In the next step, the obtained steady state solutions are employed as the initial state for the time-dependent flow model to compute the transport characteristics of the transient electroosmotic flow. Quantities such as net flow velocity and concentration transport are then investigated for different geometric and electric field parameters. In particular, the dependency of the mixing efficiency on the configuration of the electrodes and the electric input is analyzed for optimal design of the chaotic electroosmotic mixer.

2. PROBLEM DESCRIPTION AND MATHEMATICAL FORMULATION

2.1 Geometrical Configuration

A schematic of the micromixer considered in this study is illustrated in Fig. 1. This mixer combines two fluids entering from different inlets of width L_1 and L_2 into a single channel of width L_3. The fluids then enter an annular mixing chamber of inner and outer radii R_1 and R_2, respectively which is equipped by a number of microelectrodes positioned along the inner and outer walls of the annular space at angular positions of ± 45 and ± 135 degrees. Time dependent electric potential has been imposed on the electrodes which enforces the fluids to mix chaotically in the mixing chamber. Here, the fluids are manipulated via the electroosmotic slip boundary condition before they enter the outlet channel. It is assumed that the aspect ratio (channel depth to width) is large enough that the mixer can be analyzed using a two-dimensional model. The working fluid is water and each inlet has a different initial concentration value. The geometrical dimensions and material properties relevant to the model and the working fluids are given in Tables 1 and 2, respectively.

2.2 Governing Equations

The equations governing the process of mixing of the two aqueous fluids in the present electrokinetically actuated micromixer under unsteady-state condition are determined by the following three physical laws:

(i) Momentum and mass conservation is assumed to describe the flow behavior in the mixer. This leads to the Navier-Stokes equations as follows:

$$\nabla \cdot \mathbf{u} = 0 \tag{1}$$

$$\rho \frac{\partial \mathbf{u}}{\partial t} + \rho(\mathbf{u} \cdot \nabla)\mathbf{u} = \nabla \cdot \left[-p\mathbf{I} + \eta\left(\nabla \mathbf{u} + (\nabla \mathbf{u})^T\right)\right] \tag{2}$$

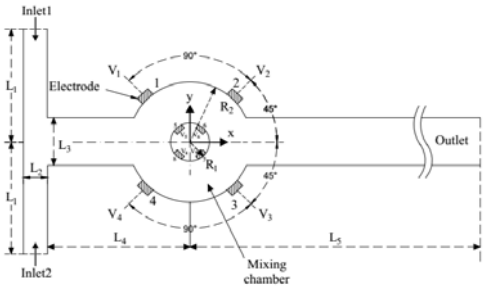

Fig. 1. Schematic of the electroosmotic micromixer.

Table 1 Geometrical dimensions

Quantity	Value (μm)
L_1	35
L_2	5
L_3	10
$L_4 = L_5 = 50$	50
R_1	5
R_2	15

Table 2 Mechanical and electrical properties of the fluid and initial values of the parameters

Parameter	Value	Unit
Density ρ	10^3	Kg/m^3
Dynamic viscosity η	10^{-3}	$Pa.s$
Relative permittivity of the fluid ε_r	80.2	-
Conductivity of the ionic solution σ	0.11845	S/m
Zeta potential ζ	–0.1	V
Amplitude of voltage applied to the electrodes V_0	0.1	V
Diffusion coefficient of the solution D	10^{-11}	m^2/s
Initial concentration of diffusing species C_0	1	mol/m^3
Frequency applied to the electrodes f	8	Hz
Mean inflow velocity U_0	0.2	mm/s

where $\mathbf{u}$ represents the fluid velocity vector, ρ the fluid density, p the pressure and η the dynamic viscosity of the fluid.

(ii) The current balance in the micromixer is described by the following diffusion equation

$$\nabla \cdot \left(\sigma \nabla V \right) = 0 \tag{3}$$

where σ is the conductivity of the ionic solution and the expression within parenthesis is the current density. Here, it has been assumed that there are no concentration gradients in the ions that carry the current and the ions in the diffuse part of the double layer are approximately in thermal equilibrium.

(iii) The convection-diffusion equation describes the concentration of the dissolved substances in the fluid according to the following equation:

$$\frac{\partial c}{\partial t} - \nabla \cdot \left(D \nabla c \right) = \lambda - \mathbf{u}.\nabla c \tag{4}$$

where c represents the concentration as a function of time, D is the diffusion coefficient, λ denotes the reaction rate, and $\mathbf{u}$ equals the flow velocity. In this model $\lambda = 0$ because the concentration is not affected by any chemical reactions. It should also be noted that for the present problem, at the upper half of the inlet the solute has a given concentration c_0, while at the lower half it is zero.

The mixing efficiency (Γ_m) is defined as follows:

$$\Gamma_m(\%) = \left(1 - \frac{\int |c - c_\infty| dx}{\int |c_0 - c_\infty| dx} \right) \times 100 \tag{5}$$

where c is the concentration value at some distance downstream (here at the outlet), c_0 is the initial concentration value before mixing the working fluids, and c_∞ is the ideal value of concentration for the completely mixed species, respectively. A fully mixed state therefore would have a 100% mixing efficiency while the unmixed state would have a 0% mixing efficiency.

2.3 Boundary Conditions

The complete system of partial differential equations governing the mixing process for the micromixer given above must be solved subject to the appropriate boundary conditions, which are discussed in this section. For the Navier-Stokes equations (1)-(2), at the inlet a laminar inflow is assumed such that

$$\mathbf{u} = -U_0 \mathbf{n} \tag{6}$$

where U_0 is the mean inflow velocity, and $\mathbf{n}$ is the outward unit normal vector to the boundary. At the outlet, a normal (zero) stress condition is adopted meaning that the mixed fluid flows freely out of the right end boundary

$$\left[-p\mathbf{I} + \eta \left(\nabla \mathbf{u} + \left(\nabla \mathbf{u} \right)^T \right) \right] \cdot \mathbf{n} = 0 \tag{7}$$

As stated earlier, a charged solution forms close to the liquid–solid interface in response to the spontaneously formed surface charge. The electric field generating the electro-osmotic flow displaces the charged liquid in the electric double layer. Assuming the double layer thickness, λ_D, is very small compared with the characteristic length, L_c, say $\lambda_D / L_c << 100$, the effect of the thin electric double layer may be represented by the Helmholtz-Smoluchowski relation between the electroosmotic velocity and the tangential component of the applied electric field. This model assumes that the velocity slips at the edge of the electric double layer. As a result, in the absence of other forces, the velocity profile eventually becomes almost uniform in the cross section perpendicular to the wall, and the fluid moves as in plug flow. In this study, we used the Helmholtz-Smoluchowski relation between the electro-osmotic velocity and the applied electric field instead of the thin, electric double-layer. Accordingly, at the mixing chamber wall, an electroosmotic velocity condition is imposed replacing the thin electric double layer with the Helmholtz-Smoluchowski equation as follows

$$\mathbf{u} = \frac{\varepsilon_0 \varepsilon_r \zeta}{\eta} \nabla_t V \quad where: \nabla_t V = \mathbf{E}_t = \mathbf{E} - \left(\mathbf{n} \cdot \mathbf{E} \right) \mathbf{n} \tag{8}$$

Where ε_r is the relative electric permittivity of the fluid, ζ the zeta potential, V the electric potential, and $\mathbf{E}$ the bulk electric field.

Note here that since variables **u** and *V* are related through the above boundary condition, the system of partial differential equations is coupled. In addition, we have neglected the slip velocity along the wall of the inlet and outlet, where no-slip boundary conditions were used, because the electric field density, which decays exponentially from the microelectrodes, is proportional to the slip velocity.

For current balance equation, i.e. Eq. (3): at the inlet, outlet and wall boundaries (except for electrode nodes), electric insulation condition is assumed

$$\nabla \cdot \left(\sigma \nabla V \right) = 0 \tag{9}$$

For electrode nodes where an AC voltage is applied, the time-dependent potentials are imposed as follows

$$V = \pm V_0 \sin\left(\omega t \right) \tag{10}$$

3) For convection-diffusion equation, i.e. Eq. (4), at the inlet, the upper half has a specified concentration c_0 whereas the lower half is set to zero. At the outlet, convective flux condition is assumed which reads

$$\mathbf{n} \cdot \left(-D \nabla c \right) = 0 \tag{11}$$

Finally, at the wall an isolating condition is imposed since there is no solution flux in that direction.

$$\mathbf{n} \cdot \left(-D \nabla c + c\mathbf{u} \right) = 0 \tag{12}$$

2.4 Solution Strategy

The mathematical model for the present design of the micromixer is contained in the set of coupled PDE's (1)-(4) in the computational domain, with boundary conditions of Eqs. (6)-(12). As there is only a one-way coupling between the electric field

and the fluid fields, it is possible to reduce the simulation time and memory requirements by

developing a special numerical strategy for solution of the system of governing equations. This strategy is based on the fact that a time-dependent electric field can be modeled as a product of a stationary electric field and a time-dependent phase factor ($\sin\omega t$). Hence, a two-step strategy for the solution process is employed as follows. In the first step, a stationary solver is developed by overriding the time-dependency of the system. In the second step, we overlook the electric currents equation and calculate the transient solution for the laminar flow and transport of diluted species equations. Then, we obtain the tangential electric field components used in the electroosmotic velocity boundary condition by multiplying the stationary DC solution by $\sin(\omega t)$.

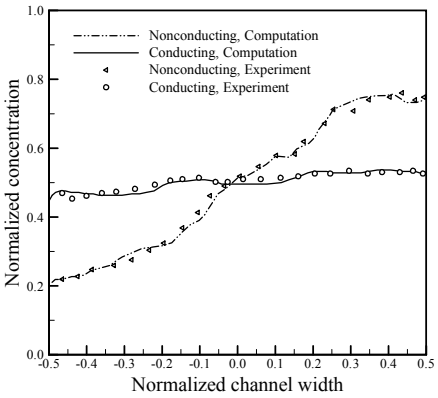

Fig. 2. Validation of the numerical simulation with the experimental data from the study of Wu and Li (2008).

3. RESULTS AND DISCUSSION

In this section, we will first summarize some considerations regarding the computational approach undertaken and then present the results obtained from the numerical simulations. The dimensionless parameters governing the present study are the Reynolds number (*Re*) and the Peclet number (*Pe*). The former gives a measure of the ratio of inertial forces to viscous forces and consequently quantifies the relative importance of these two types of forces for the given flow conditions. The latter, however, is defined as the ratio of the rate of advection of a physical quantity by the flow to the rate of diffusion of the same quantity driven by an appropriate gradient. Micromixers often deal with flows with low Reynolds and high Pe numbers, leading to slow mixing. As a result, species are often unmixed over time scales relevant to the experiments with microfluidic systems. However, mixing processes can be facilitated by reducing the characteristic length over which the diffusive mixing must occur. An efficient strategy for accelerating the mixing in such small scales is generating chaotic advection through imposing the mixing species to a time-varying electric filed, as in this study, which is capable of facilitating mixing by shortening the required diffusion length scales. This sort of

advection, however, is efficient only when the micromixer design is carefully crafted and optimized. In our study, we have $Pe = 10^2$ and $Re = 10^{-3}$, and the concentration values at the two channel inlets are 1 and 0 mol/m^3, as stated before. Two-dimensional unstructured grids were generated using the COMSOL preprocessor to analyze the micromixer performance as a function of the electrode positions. An extremely fine mesh is used in the whole flow domain to carefully capture the characteristics of the high-Pe and low-Re electroosmotic flow within the modeled micromixer. The mesh has further been refined for the areas in the vicinity of the electrodes to account for higher gradients of the quantities in these regions. In the present problem, the time scale of the unsteady electric field must be much larger than that of the transient flow in order for the Helmholtz-Smoluchowski equation to be used at the fluid-solid boundaries. This is based on the study of Cummings *et al*. (2000) who have shown that for such problems, the electric field must be at least quasi-static to neglect transient effects. In our simulations, we have set the frequency of the applied electric potential to 8 Hz, which corresponds to a time scale of the electric field 10 times larger than that of the flow, and allows for the validity of the quasi-static solution. In addition, in the presented plots, the maximum electrical voltage applied to the electrodes is considered to be V_0 .

Fig. 3. Stretching and folding behavior of the species elements.

In order to validate the numerical model used in this study for the analysis of the electroosmotic flow, we have compared our simulation results with the experimental data obtained by Wu and Li (2008) for electroosmotic flow in a T-shape micromixer with nonconducting and conducting hurdles. The mixer has two inlets at the left, connected with the anode of a DC power supply, for parallel delivery of two different chemical species. The mixing channel has a width of 300 μm . The hurdles used in the experimental study are made of silicon and have a triangular-shaped head of 200 μm in width, and 125 μm in height. Values of the diffusion coefficient and the externally applied DC electric field are 4.37×10^{-10} m^2/s and 50 V/cm, respectively. All other parameters in the simulations are set the same as in the experiment to allow for a reasonable comparison. As can be seen in Fig. 2, which compares the concentration profiles at the outlet of the micromixer between channels with conducting and non-conducting hurdles under a symmetric

arrangement, our numerical simulation results are in good agreement with the experimental data. The results also reveal that the concentration fields at the outlet in the presence of conducting hurdles become more uniform than those of the channels with nonconducting hurdles. Therefore, the flow mixing is effectively enhanced for the former case as the vortices generated near the conducting hurdles facilitate the species mixing.

Figure 3 shows the trajectories of the fluid particles passing through the central mixing chamber of the present micromixer for some typical values of the parameters discussed. As observed, the fluid particles passing through the central mixing camber experience prolonged stretching and folding due to strong influence of the time-varying electrokinetic actuation applied through the electrodes. Stretching results in nearby points diverging, folding results in distant points being mixed together. The set of stretching and folding of lines observed here in the mixing chamber is usually the fundamental requirement for effective chaotic mixing. This electrokinetic excitation along with the natural splitting and recombination effect of the mixing chamber on the working fluids facilitates the final stage of mixing through both advection and molecular diffusion.

A variety of case studies and mixing results can be achieved based on different positioning of the electrodes. In the present study, three different electrode configurations are examined based on the number and arrangement of the electrodes on the inner and outer loops of the mixing chamber. The electric potentials applied on each individual case is as follows: case 1 with $V_1 = -V_2 = V_3 = -V_4 = V_0 \sin(\omega t)$ and $V_5 = V_6 = V_7 = V_8 = 0$; case 2 with $V_1 = -V_2 = V_3 = -V_4 = V_5 = -V_6 = V_7 = -V_8 = V_0 \sin(\omega t)$; and case 3 with $V_1 = V_2 = V_3 = V_4 = V_0 \sin(\omega t)$ and $V_5 = V_6 = V_7 = V_8 = -V_0 \sin(\omega t)$. The first case (Case 1) is the original design proposed by Chen *et al.* (2003) and Zhang *et al.* (2004) based on placement of only four electrodes on the outer loop of the mixing chamber. The designs in Cases 2 and 3 are introduced in this study to demonstrate the effect of an increase in the number of the electrodes as well as the importance of electrode configuration selection for the design. As mentioned before, smaller mesh sizes have been selected for the areas near the electrodes which allows for precisely capturing the sudden changes in the values of the quantities within these regions.

Figures 4 through 7 present the simulation results for these cases, including electric potential contours, mass concentration contours, and distribution of streamlines as well as velocity vectors at the time corresponding to the maximum value of the applied electric potential ($t = 1.9063$). In addition, Figs. 8 through 11 illustrate spatial and temporal variations of the concentration and the average value of this quantity. Figure 4 presents the potential contour and the electrode configuration for the three test cases considered in this study. As shown, the maximum value of the electric potential applied on the electrodes is V_0. In addition, the other non-electrode sections of the first micromixer have zero electric potential. The position of the electrodes changes from one case to another, and the electrode potentials vary with time in a sinusoidal manner. The streamlines and velocity vectors for the above-mentioned cases at the time corresponding to the peak value of the alternating current voltage applied ($t = 1.9063$) are illustrated in Figs. 5 and 6, respectively. The general trend observed here for all the cases investigated is that after the two fluids flow uniformly from different entrances of the T-shape micromixer, they meet up and the unified flow streams towards the annularmixing chamber and undergoes the transient

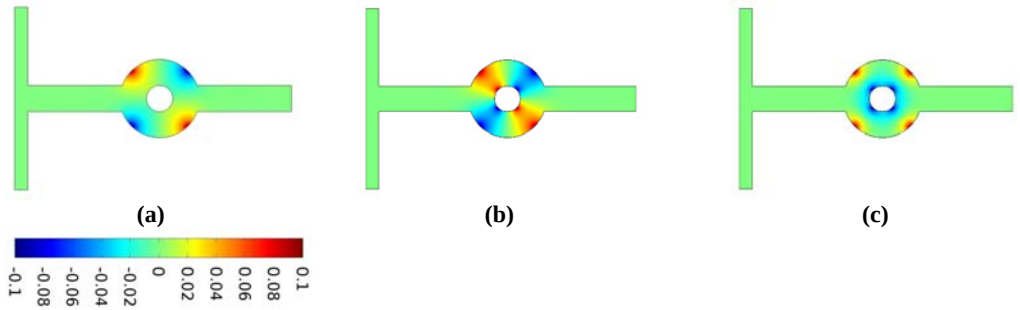

Fig. 4. The electrode configurations and potential contours for the case studies considered in this study: (a) Case 1; (b) Case 2; (c) Case 3; (d) Case 4.

Fig. 5. Illustration of the streamlines for different case studies at the time corresponding to the peak value of the alternating current voltage applied (t = 1.9063): (a) Case 1; (b) Case 2; (c) Case 3.

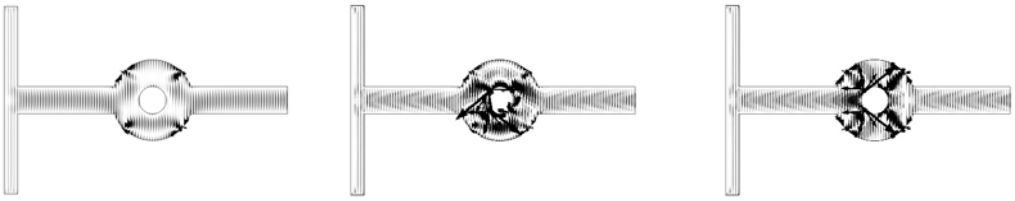

(a) **(b)** **(c)**

Fig. 6. Velocity vectors for different case studies at the time corresponding to the peak value of the alternating current voltage applied (t = 1.9063): (a) Case 1; (b) Case 2; (c) Case 3.

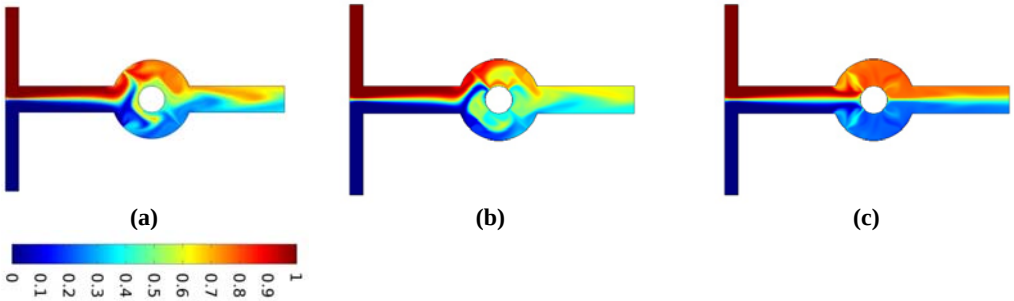

(a) **(b)** **(c)**

Fig. 7. Distribution of the concentration for different case studies at the time corresponding to the peak value of the alternating current voltage applied (t = 1.9063): (a) Case 1; (b) Case 2; (c) Case 3.

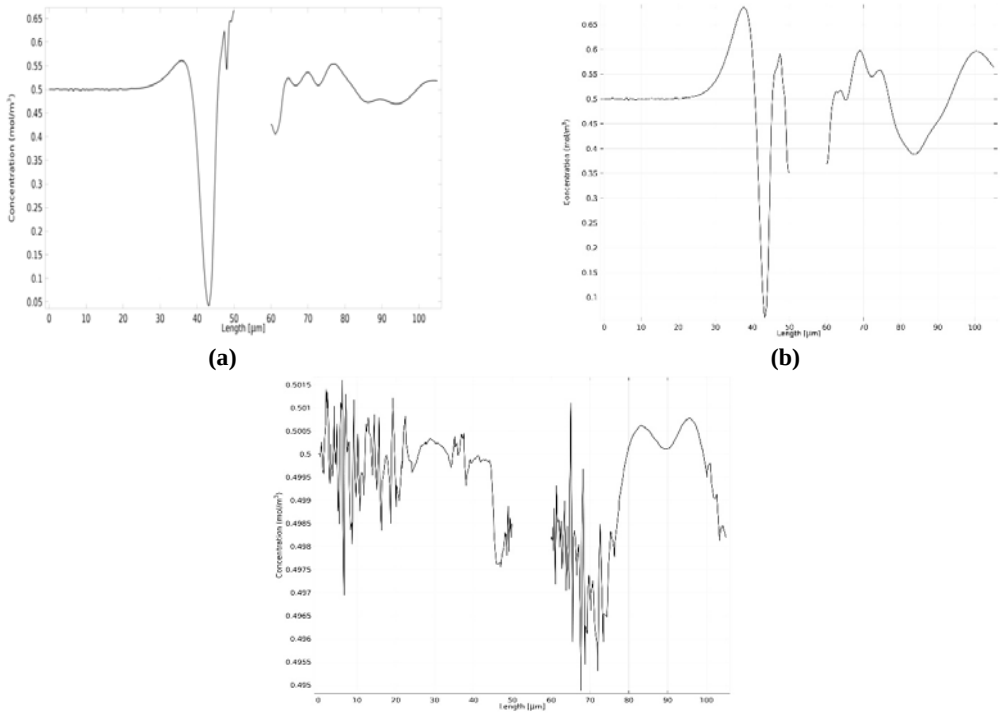

(a) **(b)**

(c)

Fig. 8. Variation of the concentration of the mixture along the horizontal axis of the micromixers at the time corresponding to the peak value of the alternating current voltage applied (t = 1.9063): (a) Case 1; (b) Case 2; (c) Case 3.

condition in there caused by the applied AC potentials. The flow then moves towards the microelectrodes under the influence of the applied electric potentials and is strongly stirred by electroosmotic recirculation formed around the electrodes. As a result, the individual streamlines near the electrodes move along upper/lower wall of the mixing chamber. When these streamlines meet with the opposite flows at the lower/upper part of the chamber, eddy rotations form near each electrode and a number of vortices appear in the annular mixing space. This increases the velocity of fluid particles in zones near the electrodes and makes the fluid particles stay in the central loop stretched and folded for a long time before they enter the outlet channel. Moreover, it was observed that because of the exponentially increased electric field near the electrodes, the eddy velocity is faster near the electrodes. The applied sinusoidal voltage causes

the streamlines to become concentrated and vortices start to form near each electrode. In addition, as the voltage of the electrodes increases, several vortices form near the walls of the mixing chamber where the electrodes are placed. A comparison between the streamlines and velocity vectors for the three test cases considered here reveals that in case 2 for which eight electrodes are installed on both the inner and other loops in a cross-like pattern (electrodes with the same potential are positioned on one branch of a cross sign), stronger vortices are observed and the flow is stirred more vigorously.

In Fig. 7, distribution of the concentration of the mixture for the three cases with different positioning of the microelectrodes is demonstrated. The horizontal colormap below the plot denotes the high and low limits of the concentrations values; with C = 0.5 being the completely mixed state and C = 0 or 1 showing the initial unmixed state. At first, the two fluids have the initial concentrations of zero/unity as they flow uniformly from the lower/upper entrances of the micromixer towards the mixing chamber. when the two fluid streams flow through the mixing chamber, the device continuously applies a time-varying electric field and a resulting electroosmotic force to the working fluid which induces electrokinetic perturbation to the working fluids. As a result of this perturbation, the laminar pressure-driven flow is extensively pushed up and down at the mixing chamber, and the flow particles undergo a stochastic stretching/folding process. This induces

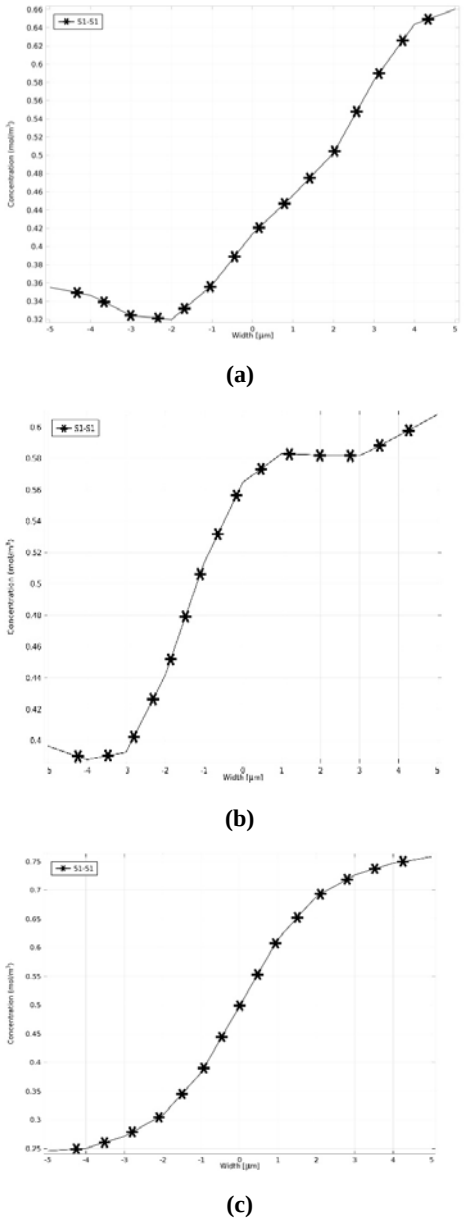

(a)

(b)

(c)

Fig. 9. Variation of the concentration of the mixture across the micromixers outlets at the time corresponding to the peak value of the alternating current voltage applied (t = 1.9063): (a) Case 1; (b) Case 2; (c) Case 3.

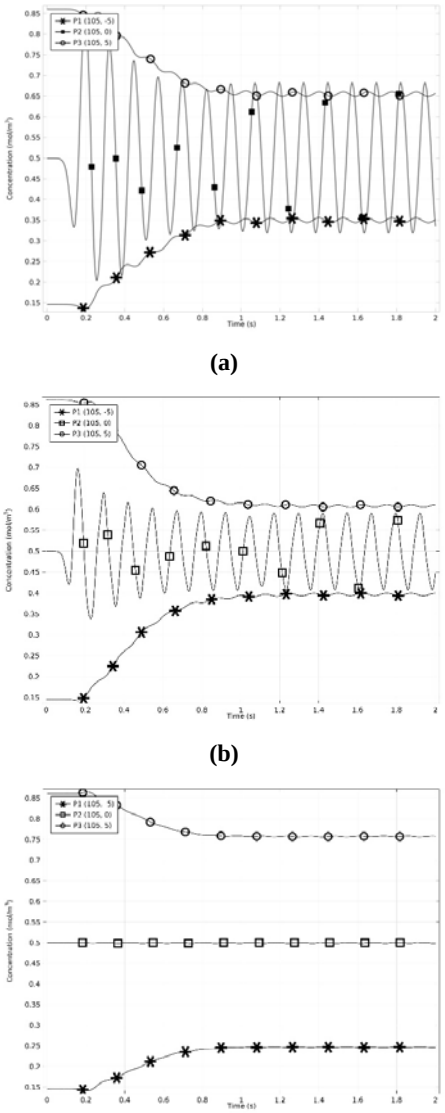

(a)

(b)

(c)

Fig. 10. Time history of concentration variation for three control points at the lower, middle, and upper parts of the outlet section of the micromixers: (a) Case 1; (b) Case 2; (c) Case 3.

a number of vortices within the annular mixing space which circulate the liquids from the high-concentration zone to the low-concentration area, and vice versa. As a result, the mixture tends towards becoming fully homogenized within the mixing chamber. Note here that the number of vortices differs from case to case, and different arrangements could result in a variety of vortex formations. It can be inferred

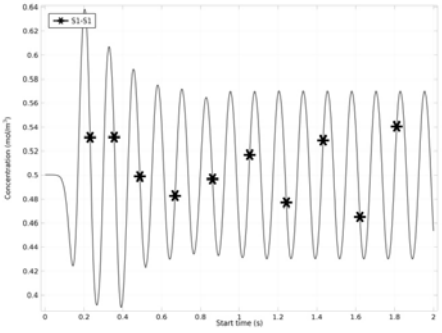

(a)

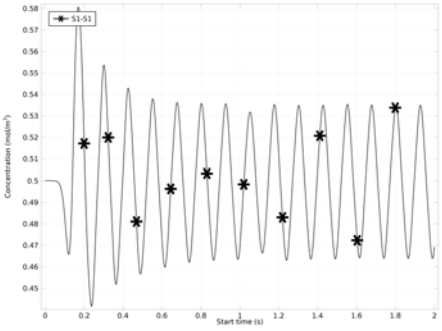

(b)

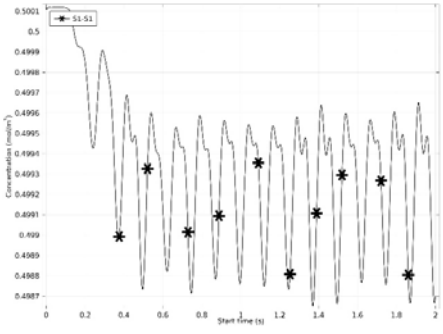

(c)

Fig. 11. Time history of variation of the average concentration at the outlet section of the micromixers: (a) Case 1; (b) Case 2; (c) Case 3.

from the results that the design associate with Case 2 presents a better mixing result compared to the other designs as the concentration of the output mixture obtained from the corresponding micromixer has less deviation from an ideal mixture. This could mainly be attributed to the fact that the size of the circulation zones is larger for this case in comparison with the other cases. The observation in turn, implies that the induced-charge electrokinetic phenomenon around the annular space caused by the electrode arrangement in Case 2 leads to more significant changes to the flow field and concentration transport compared to the other cases. Hence, the corresponding mixing efficiency is expected to be higher for this case. An investigation into history of the transient behavior of the mixing process for all the case studies (not shown here for saving space) also revealed that as the applied voltage is increased sinusoidally from zero to the maximum value of V_0, a number of vortex zones in the vicinity of the electrodes are

Table 3 Mixing efficiency for the cases under consideration

	Case number		
	1	2	3
Γ_m	82.9%	91.5%	49.2%

generated which increase the velocity of fluid particles. Also, the increase in the potential significantly changes the size of the flow recirculation which remarkably provokes stretching and folding of the elements of the mixing agents.

Figures 8 through 11 represents a series of results illustrating the concentration profiles of the confluent stream in the mixing chamber and connecting channel. Among the plots depicted are the variation of the concentration of the mixture along the horizontal axis of the micromixers (Fig. 8) and the concentration of the resulting mixture at the exit of the microchannel across the channel width as a representative of the mixing efficiency or performance of the micromixers (Fig. 9), both at the time corresponding to the peak value of the alternating current voltage applied; i.e., at $t = 1.9063$. Moreover, three points at the lower $\left(P_1(105,-5)\right)$, middle $\left(P_2(105,0)\right)$, and upper $\left(P_3(105,5)\right)$ parts of the outlet section of the micromixers are considered as control points, and time history of variation of their concentrations is demonstrated (Fig. 10). Also, time history of variation of the average concentration over the outlet cross section is presented (Fig. 11). Finally, the values of the mixing efficiency, Γ_m, for the three designs are provided in Table 3. Inclusively going through the results, it is perceived that the transient conditions governing the mixing procedure within the annular chamber has significant effects on the whole process of mixing as well as the performance of the micromixer. The results also confirm that even after the mixing species leave the mixing chamber, which is the only section equipped with the microelectrodes and under direct influence of the applied electric field, the unsteady effects persist within the rest part of the micromixer and appear to continuously influence the confluent stream up to the exit section. However, generally speaking, the effect of the transient conditions on the mixing process is less experienced as the mixture escapes the annular chamber and approaches the output. The results once again confirm that the design based on disposition of eight microelectrodes on both the inner and outer

loops of the mixing chamber in a cross-like pattern (Case 2) gives the best performance among the three cases investigated in this study. The evidence for this conclusion are more ideal values of the concentration for the resulting mixture associated with the design of Case 2 as well as less temporal and spatial deviation in the quality of the mixing products for this case compared with the other designs. In fact, it is deduced that for Case 2, the resulting chaotic advection and electroosmotic recirculation of the fluid due to continuous application of the time-dependent actuation helps the mixture to effectively homogenize within the mixing chamber. As a final point in the present study, our simulation results also reveal that increasing the number of the electrodes from four to eight and thereby, increasing the applied external potential does not necessarily lead to improved functionality or performance of the present micromixer. To clarify, it is seen that although the designs associated with Cases 2 and 3 share the same number of microelectrodes (eight electrodes), the quality of the mixing products is different for these cases so that in comparison with the design in Case 1 (with four electrodes), the former/latter case presents a better/worse mixing performance. This clearly shows that besides the number of the electrodes, their arrangement is a very influential factor in determining the optimal design for the present electroosmotic micromixer.

4. CONCLUSIONS

In this study, an electrokinetically actuated, active T-type micromixer with an annular mixing chamber and different electrode arrangements is investigated numerically to demonstrate the effect of electrode configuration on the resulting mixing performance. A spatially and temporally varying electric field is imposed on the working fluids by microelectrodes, and the impact of electrode position on the flow and concentration fields is studied. The concentration surface plot, fluid streamlines, and electric potential lines for different electrode arrangements are then presented. In an attempt to find the optimized performance of the micromixer, the mixing performance is evaluated by investigating potential effects of electrode configuration and the number of electrodes in the mixing chamber on the overall mixing performance. The results from this study can meaningfully contribute to development of efficient and low-cost electrokinetic micromixers for applications such as transporting, mixing, separating, and manipulation of various molecular or colloidal entities e.g. DNA, protein, polymers, etc. in microfluidic chips. Moreover, the simplicity in the design of the optimized micromixer makes its fabrication and control feasible.

REFERENCES

Baheri Islami, S. and M. Khezerloo (2017). Enhancement of Mixing Performance of Non-Newtonian Fluids using Curving and Grooving of Microchannels. *Journal of Applied Fluid Mechanics* 10, 127-141.

Biddiss, E., D. Erickson, and D. Li (2004). Heterogeneous surface charge enhanced micromixing for electrokinetic flows. *Analytical Chemistry* 76, 3208-3213.

Boy, A. and B. D. Storey (2007). Electrohydrodynamic instabilities in microchannels with time periodic forcing. *Physical Review E* 76, 026304 (11 pages).

Campisi, M., D. Accoto, F. Damiani, and P. Dario (2009). A soft-lithographed chaotic electrokinetic micromixer for efficient chemical reactions in lab-on-chips. *Journal of Micro-Nano Mechatronics* 5, 69-76.

Chen J. K., C. N. Weng, and R. J Yang (2009). Assessment of three AC electroosmotic flow protocols for mixing in microfluidic channel. *Lab on a Chip* 9, 1267-1273.

Chen, H., Y. T. Zhang, I. Mezic, C. D. Meinhart, and L. Petzold (2003), Numerical simulation of an electroosmotic micromixer, *Proceedings of Microfluidics 2003 (ASME IMECE)*, 1-6.

Cummings, E., S. Griffiths, R. Nilson and P. Paul (2000), Conditions for similitude between the fluid velocity and the electric field in electroosmotic flow, *Analitica Chemistry* 72, 2526-2532.

Paul (2000), Conditions for similitude between the fluid velocity and the electric field in electroosmotic flow, *Analytical Chemistry* 72, 2526-2532.

Daghighi, Y. and D. Li (2013). Numerical study of a novel induced-charge electrokinetic micro-mixer. *Analytica Chimica Acta* 763, 28-37.

Glasgow, I. and N. Aubry (2003). Enhancement of microfluidic mixing using time pulsing. *Lab on a Chip* 3, 114-120.

Huang, S. H., S K. Wang, H. S. Khoo, and F. G. Tseng (2007). AC electroosmotic generated in-plane microvortices for stationary or continues fluid mixing. *The 14th International Conference on SolidState Sensors, Actuators and Microsystems*, Lyon, France, 1349-1352.

Jacobson, S. C., E. E. McKnight, and J. M. Ramsey (1999). Microfluidic devices for electrokinetically driven parallel and serial mixing. *Analytical Chemistry* 71, 4455-4459.

Jain, M., A. Yeung, and K. Nandakumar (2009). Efficient micromixing using induced-charge electroosmosis. *Journal of Microelectromechanical Systems* 18, 376-384.

Karniadakis, G., A. Beskok, and N. Aluru (2005) *Micro flows and nano flows: fundamentals and simulation*. Springer, New York.

Lee, C. Y., C. L. Chang, Y. N. Wang, and L. M. Fu (2011). Microfluidic mixing: A review. *International Journal Molecular Sciences* 12, 3263-3287.

Li, P., J. Cogswel, and M. Faghri (2012). Design

and test of a passive planar labyrinth micromixer for rapid fluid mixing. *Sensors and Actuators B: Chemical* 174, 126-132.

Lim, C. Y., Y. C. Lam, and C. Yang (2010). Mixing enhancement in microfluidic channel with a constriction under periodic electro-osmotic flow. *Biomicrofluidics* 4, 014101 (18 pages).

Mao, H., T. Yang, and P. S. Cremer (2002). A microfluidic device with a linear temperature gradient for parallel and combinatorial measurements. *Journal of American Chemistry Society* 124, 4432-4435.

Ng, W. Y., Sh. Goh, Y. Ch. Lam, Ch. Yang, and I.R. Rodriguez (2009). DC-biased AC-electroosmotic and AC-electrothermal flow mixing in microchannels. *Lab on a Chip* 9, 802-809.

Nguyen, N. T. and Z. Wu (2005). Micromixer-A review. *Journal of Micromechanics and Microengineering* 15, 1-16.

Oddy, M. H., J. G. Santiago and J. C. Mikkelsen (2001). Electrokinetic instability micromixing. *Analytical Chemistry* 73, 5822-5832.

Olesen, L. H., H. Bruus, and A. Ajdari (2006). Ac electrokinetic micropumps: The effect of geometrical confinement, Faradaic current injection, and nonlinear surface capacitance. *Physical Review E* 73, 056313 (16 pages).

Park, B. O. and S. Song (2012). Effects of multiple electrode pairs on the performance of a micromixer using dc-biased ac electro-osmosis. *Journal of Micromechanics and Microengineering* 22, 1-6.

Qian, S. and H. H. Bau (2005). Magnetohydrodynamic flow of RedOx electrolyte. *Physics of Fluids* 17, 067105 (12 pages).

Qian, S. and H. H. Bau (2009). Magneto-hydrodynamics based microfluidics. *Mechanics Research Communications* 36, 10-21.

Qian, S., J. Zhu, and H. H. Bau (2002). A stirrer for magnetohydrodynamically controlled minute fluidic networks. *Physics of Fluids* 14, 3584-3592.

Ramos, A., A. Gonzalez, A. Castellanos, N. G. Green, and H. Morgan (2003). Pumping of liquids with ac voltages applied to asymmetric pairs of microelectrodes. *Physical Review E* 67, 056302 (11 pages).

Sasaki, N., T. Kitamori, and H. B. Kim (2010). Experimental and theoretical characterization of an AC electroosmotic micromixer. *Analytical Sciences* 26, 815-819.

Stevens, J., G. Brossard, A. Blom, A. Douteur, and Y. Delmotte (2012). A Novel Sintered Porous Micromixer for the Effective Mixing of Biologics and Scale Model Investigation of Micromixing Mechanisms. *Journal of Applied Fluid Mechanics* 5, 91-100.

Stoeber, B., D. Liepmann, and S. J. Muller (2007). Strategy for Active Mixing in Microdevices. *Physical Review E* 75, 066314 (4 pages).

Sudarsan, A. and V. Ugaz (2006). Fluid mixing in planar spiral microchannels. *Lab on a Chip* 6, 74-82.

Suh, Y. K. and S. Kang (2010). A review on mixing in microfluidics. *Micromachines* 1, 82-111.

Tofteberg, T., M. Skolimowski, E. Andreassen, and O. Geschke (2010). A novel passive micromixer: Lamination in a planar channel system. *Microfluidics and Nanofluidics* 8, 209-215.

Wu, Z. and D. Li (2008). Micromixing using induced-charge electrokinetic flow. *Electrochimica Acta* 53, 5827-5835.

Wu, Z. and D. Li (2008a). Mixing and flow regulating by induced-charge electrokinetic flow in a microchannel with a pair of conducting triangle hurdles. *Microfluidics and Nanofluidics* 5, 65-76.

Wu, Z. and D. Li (2008b). Micromixing using induced-charge electrokinetic flow. *Electrochimica Acta* 53, 5827-5835.

Xuan, X. and D. Li (2004). Analysis of electrokinetic flow in microfluidic networks. *Journal of Micromechanics and Microengineering* 14, 290-298.

Yang, Z., S. Matsumoto, H. Goto, M. Matsumoto, and R. Maeda (2001). Ultrasonic micromixer for microfluidic systems. Sensors and Actuators A: Physical 93, 266-272.

Ye, C. and D. Li (2004). 3-D transient electrophoretic motion of a spherical particle in a T-shaped rectangular microchannel. Journal of Colloid and Interface Science 272, 480-488.

Zhang, Y. T., H. Chen, I. Mezic, C. D. Meinhart, L. Petzold, and N.C. MacDonald (2004), SOI processing of a ring electrokinetic chaotic micromixer, *NSTI Nanotechnology Conference and Trade Show* 1, 292-295.

Zhu, X. and E. S. Kim (1997). Acoustic-wave liquid mixer, in Microelectromechanical Systems (MEMS); Dynamic Systems and Control Division (DSC). *American Society of Mechanical Engineers: Fairfield* 62, 35-38.